

Perspective

Electrocapillary boosting electrode wetting for high-energy lithium-ion batteries

Hao Cui,¹ Youzhi Song,^{1,*} Dongsheng Ren,¹ Li Wang,^{1,*} and Xiangming He^{1,*}

SUMMARY

Large, thick, and highly pressed electrodes are desirable for high-energy lithium-ion batteries (LIBs), as they help to reduce the mass ratio and cost of the inert materials. However, this energy-density-oriented electrode technology sets new challenges for electrolyte filling and electrode wetting, which profoundly limits the production efficiency and battery performance. In this perspective, we pioneer and document well the proposal of accelerating electrode wetting via electrocapillary. First, the fundamental principles of electrode wetting, as well as characterization approaches including conventional surface analysis, electrochemical methodologies, and *in situ* spectroscopic imaging techniques, are outlined. Then, the fundamentals of electrocapillarity and the key elements (electrodes, electrolytes, and voltages) involved in electrocapillarity are carefully reviewed. In addition, the feasibility of employing electrocapillarity to boost electrode wetting is discussed according to the Lippmann equation. Moreover, the effect of electrocapillarity on promoting battery filling is successfully verified using commercial 3.1 Ah LiFePO₄ (LFP)/graphite (Gr) pouch cells. Ultrasonic imaging indicates that the sample subjected to the electrocapillary effect is completely wetted within 2 h, whereas the control sample remains incompletely wetted even after 5 h. This work is meaningful for efficient battery manufacturing by providing a novel strategy to accelerate battery filling.

INTRODUCTION

Due to the high energy conversion efficiency and high energy density, lithium-ion batteries (LIBs) are widely used as portable, mobile, and stationary energy storage devices, and their applications have radically revolutionized human society.¹ Currently, the battery industry is committed to further improving the energy density of LIBs to meet the ever-increasing demands through either new electrode materials or optimized battery design/manufacturing technology.² The US Department of Energy (DOE) set an energy density target of 350 Wh kg⁻¹ for the next-generation LIBs for electric vehicles (EVs) by 2030.³ Apart from employing chemical materials with high-specific capacity, the optimized design of the physical structure also plays an important role in upgrading the practical energy density of LIBs.⁴ Large size, thick, and highly pressed electrodes are desirable for LIBs that have high energy density (>300 Wh Kg⁻¹) because they help to reduce the mass share of inert materials and cost. For example, as early as 2014, Wood III et al. had suggested that by doubling the thickness of electrodes could increase the energy density of a LiNi_xMn_yCo_{1-x-y}O₂ (NMC)/graphite (Gr) battery by 17% while reducing the cost by 31%.⁵ Recently, new concepts in cell-to-pack (CTP) have been introduced to improve the energy density of individual batteries and packs, such as the blade

CONTEXT & SCALE

Increasing the proportion of active materials through thick, large, and high-pressure-density electrodes is an important way to increase the energy density of lithium-ion batteries beyond innovations in battery chemistry, but this poses substantial challenges for electrolyte infiltration through porous electrodes. Under such a background, promotion strategies to enhance battery wetting are analyzed based on the wettability theory of porous electrodes and the Washburn equation. As an emerging method, electrowetting is creatively proposed, analyzed, and employed to promote electrode wetting during battery infiltration. Potential regulation to enhance electric interactions between the electrode and electrolyte is confirmed to be effective in producing fast and uniform electrode wetting. Moreover, the advantages and feasibility for electrowetting management through voltage regulation support the high-quality battery products.

battery from Build Your Dreams (BYD) company Ltd. The lithium iron phosphate (LiFePO₄ (LFP))-based blade battery improves the energy density of pack from 110 to 175 Wh kg⁻¹ with the help of highly pressed thicker electrodes.⁶ Strikingly, Li et al. reported a millimeter-thick LiCoO₂ cathode with a thickness of up to 800 μm.⁷ Nevertheless, the energy-density oriented electrode technology has presented new challenges for electrolyte filling and electrode wetting (Figure 1), which profoundly limits the production efficiency and battery performance.⁸

Generally, LIBs consist of porous electrodes and membrane separators sandwiched together, and the thickness and compactness of the electrode are much higher than that of the separator.⁹ The pores in the electrode, which have a porosity of approximately 20%–40%, need to be wetted and filled with liquid electrolyte to allow free Li⁺ transfer.¹⁰ Nevertheless, electrolyte accessibility and wettability in the highly pressed electrodes are emerging challenges.¹¹ On the one hand, the increased electrode area, thickness, and calendar density dramatically increase the diffusion distance and resistance during electrolyte wetting. On the other hand, the high stacking density of the electrodes not only increases the time required for battery filling and reduces battery productivity but also brings new challenges for quality control of LIBs.¹² Furthermore, the incompletely wetted electrodes can lead to high local current densities around the electrochemically active particles,¹³ inhibit the formation of a uniform solid electrolyte interphase (SEI),¹⁴ and accelerate parasitic reactions and lithium precipitation,¹⁵ thus resulting in limited capacity, low Coulombic efficiency,¹⁶ and rapid decay.¹⁷ Many efforts have been made to accelerate battery filling and wetting by means of vacuum assistance, warm resting, addition of wetting agents,¹⁸ and designing electrode architectures.⁴ In addition, some imaging techniques—including transmission neutron,¹⁹ X-ray imaging,²⁰ ultrasonic imaging,²¹ locked thermography experiments,²² and numerical simulations²³—have also been applied to study the infiltration of electrolytes in porous electrodes. However, the actual outcomes of these approaches are insufficient and limited in case of highly pressed thick electrodes. Therefore, it is very imperative and significant to deeply understand the infiltration behavior and provide a sound technology to accelerate infiltration in high-energy batteries.

A recent work revealed a remarkably close correlation between the process of electrolyte wetting and the evolution of open circuit voltage (OCV) of a battery.²⁴ It inspires the possibility of accelerating the infiltration by applying an external voltage, that is, electrocapillary. Electrocapillary, or electrowetting effect, is a phenomenon where the wetting of the liquid electrolyte on the electrode surface is modulated by the applied electrical potential, in which the interactions between ions (anions and cations) in the electrolyte and the electrode surface are changed due to the additional potential.²⁵ Based on this phenomenon, digital microfluidics,²⁶ optical switchable lenses,²⁷ and electronic displays²⁸ have been rapidly developed and commercialized in recent years. Considering the fact that a battery configuration also involves electrodes, liquid electrolyte (lithium salts dissolved in organic solvents), and OCV, which exactly matches the application scenario of electrowetting, it is reasonable to deduce that electrowetting has the potential to be used to accelerate the electrolyte wetting in high-energy LIBs.

In this perspective, we emphasize the feasibility of electrocapillary to accelerate the electrode wetting inside high-energy batteries. First, the fundamentals and characterization approaches, as well as current promoting strategies for the electrode wetting of LIBs, are outlined. Second, the mechanisms of electrocapillary are briefly overviewed, and its potential for being applied in high-energy batteries is

¹Institute of Nuclear and New Energy Technology, Tsinghua University, Beijing 100084, China

*Correspondence: syouzhi@126.com (Y.S.), wang-l@tsinghua.edu.cn (L.W.), hexm@tsinghua.edu.cn (X.H.)

<https://doi.org/10.1016/j.joule.2023.11.012>

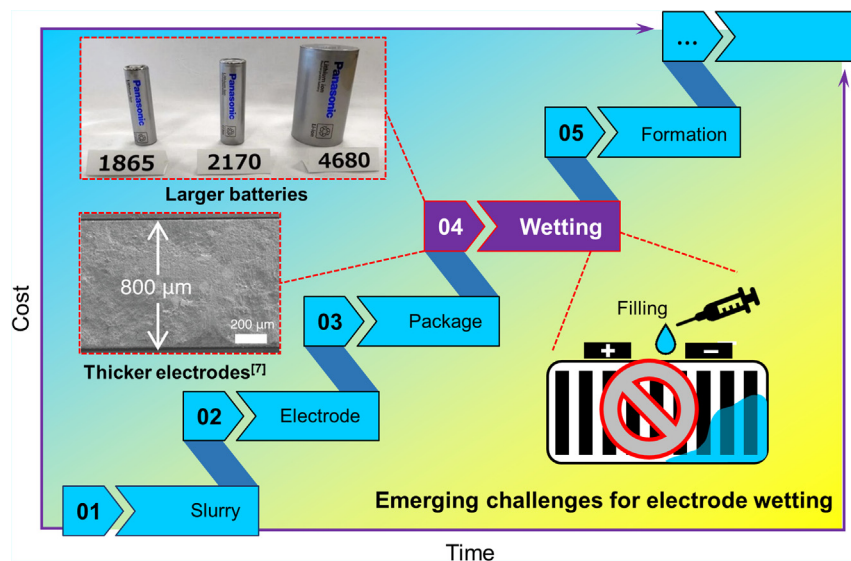


Figure 1. Electrode wetting is emerging as a key challenge in the production of high-energy LIBs Large, thick, and highly pressed electrodes are desirable for high-energy lithium-ion batteries (LIBs), as they help to reduce the mass ratio and cost of the inert materials. However, this energy-density-oriented electrode technology sets new challenges for electrolyte filling and electrode wetting, which profoundly limits the production efficiency and battery performance. SEM image of the 1 mm-thick LiCoO_2 cathode. Adapted with permission.⁷ Copyright 2023, Science.

prospected. Finally, the effectiveness of electrowetting in the battery-wetting process is further experimentally verified by applying external voltages on commercial 3.1 Ah LFP/Gr pouch cells.

FUNDAMENTALS OF ELECTRODE WETTING

In practical LIBs, especially those with high energy density, electrodes are characterized with high compression density, nonuniform pore size, high tortuosity, high thickness, and random pore distribution. Besides, the active material, binder, and carbonous conductors vary greatly in surface energy. All of these features present substantial challenges for electrode wetting and detection methods. Therefore, it is critical to conduct studies on the wetting mechanisms in LIBs.

General mechanism of electrode wetting

The filling is a wetting issue between the liquid electrolyte and porous electrode and is essentially determined by the interactions between these two components (Figure 2). The wettability of solid surfaces is an old and frequently revisited topic that impacts most fields of science and technology throughout development processes.³¹ In the case of a given solid and liquid, the droplet on a solid surface shows concrete characteristics due to the specific interactions between the solid and liquid, and the angle formed between the tangential line of the liquid-solid contact edge and the solid plane is defined as the contact angle.³² As a classical theory on the wetting relationship between solids and liquids, the contact angle θ is a macroscopic and direct natural parameter that characterizes the wettability of solid surfaces by liquids.²⁹ Although the actual wetting behavior of droplets on solid surfaces is dynamic and is influenced by the roughness and local chemistry of the solid surface, it is common to only consider the apparent equilibrium contact angle. In an ideal wetting situation, in which the solid surface is chemically homogeneous, atomically

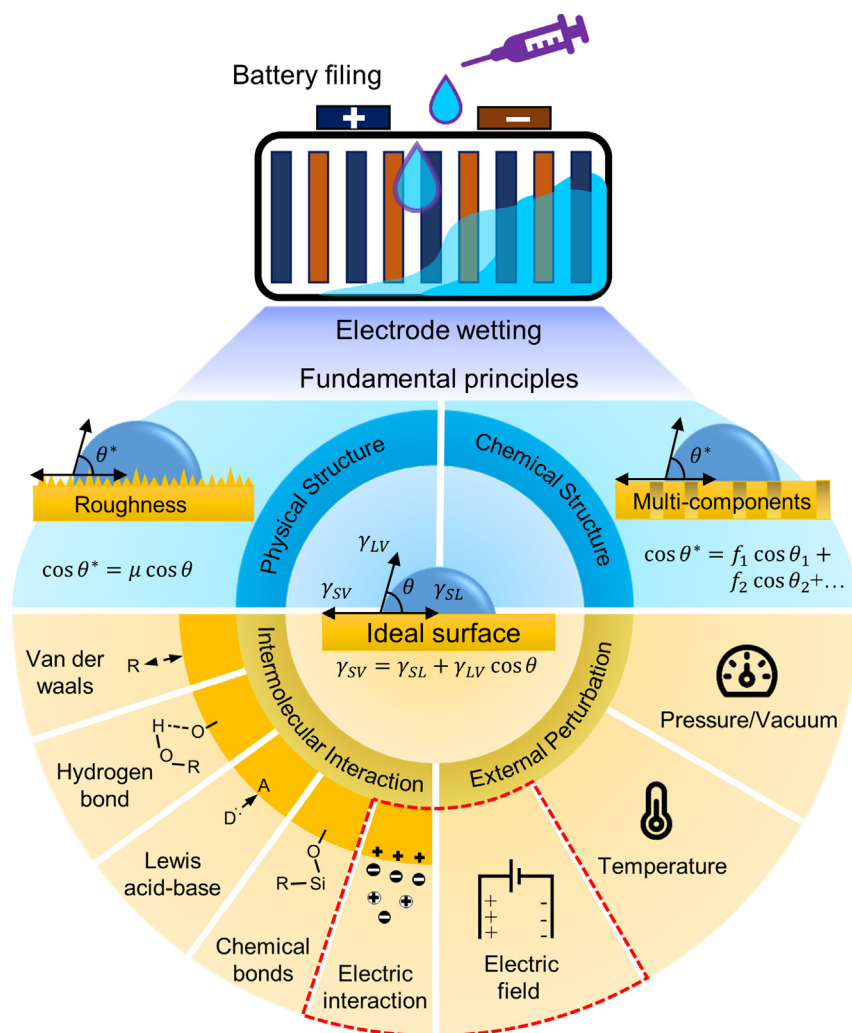


Figure 2. An overview of electrode wetting and related fundamental principles

As a classical theory on the wetting relationship between solids and liquids, the contact angle θ is a macroscopic and direct natural parameter that characterizes the wettability of solid surfaces by liquids.²⁹ However, the actual surface of porous electrodes varies greatly from an ideal solid surface. The physical microscope structure or chemical topological differences in active material particles influence the contact angle of electrolytes,³⁰ whereas the interaction between solid surface and liquid molecules can lead to different wettability in porous electrodes. In addition, external perturbations exert integrated effects on the electrolyte-wetting process, although changing in the contact angle.

flat, and not changing during contact, Neumann-Young's equation shown below expresses the relationship between the contact angle and interfacial tension³³:

$$\gamma_{SV} = \gamma_{SL} + \gamma_{LV} \cos \theta \quad (\text{Equation 1})$$

where γ_{SV} , γ_{SL} and γ_{LV} are the solid-vapor, solid-liquid, and liquid-vapor interfacial tensions, respectively.

However, the actual surface of porous electrodes varies greatly from an ideal solid surface. The physical microscope structure or chemical topological differences in active material particles influence the contact angle of electrolytes,³⁰ whereas the interaction between solid surface and liquid molecules can lead to different

wettability in porous electrodes (Figure 2). In addition, external perturbations exert integrated effects on the electrolyte-wetting process, although with changes in the contact angle. Based on these different factors, the contact angle of an electrode material and improvement strategies for electrolyte wetting have been studied in depth.

To describe the effect of physical defects on electrode particle wettability, Wenzel's model can be utilized for the actual macroscopic contact angle θ^* below³⁴:

$$\cos \theta^* = \mu \cos \theta \quad (\text{Equation 2})$$

The parameter μ represents the roughness, which is defined by the ratio of the real rough surface area and the projected surface area. Considering that the roughness μ is usually higher than 1 and with an upper limit lower than 2, the specific hydrophilic or hydrophobic nature is higher than that predicted by Wenzel's model. In addition, the topological structure of chemical variations from multiple components on the electrode solid surface can affect the contact angle based on the Cassie-Baxter model, as shown in the equation below³⁵:

$$\cos \theta^* = f_1 \cos \theta_1 + f_2 \cos \theta_2 + f_i \cos \theta_i + \dots \quad (i = 1, 2, 3 \dots) \quad (\text{Equation 3})$$

where f_i and θ_i are the fraction and contact angle of a specific component within the complex composition of electrode materials.

Although the physical topography and chemical component distribution of electrode material surfaces have an influence on electrolyte wetting, the intermolecular interactions between solid surface atoms and various electrolyte components, such as solvent molecules, anions, and cations, are intrinsic factors influencing solid-liquid interface wettability.³⁶ Among the numerous component combinations of the active material surface and electrolytes, the interactions include van der Waals forces, hydrogen bonds, Lewis acid-base interactions, and even chemical bonds.³⁷ In addition, external perturbations can change the wettability of electrolytes by modifying the interactions of electrolytes and electrodes.³⁶ The combined effects of the external field and molecular features of porous electrodes and electrolytes present significant possibilities for improving the electrode-wetting process. First, mechanical disturbance methods, such as increasing the injection pressure and creating a vacuum environment, can significantly improve the infiltration process of porous electrodes. In addition, moderately increasing the temperature helps to enhance the electrolyte-wetting process of different cells. Furthermore, based on electrocapillary theory, the electric field has a regulating effect on liquid wetting on the solid surface by tuning the surface charge state of the electrode particles.³⁸

Characterization of electrode wetting

To gain insight into electrolyte-wetting characteristics, a variety of characterizations have been performed on the wetting behavior of porous electrodes inside LIBs. Briefly, they can be classified as conventional characterizations, electrochemical methods, *in situ* spectroscopic imaging techniques, and numerical simulations (Figure 3).

Conventional characterizations

Characterizations of the surface morphology and chemical properties by scanning electron microscopy (SEM), X-ray photoelectron spectroscopy (XPS), and energy dispersive spectrometry (EDS) have helped to elucidate the mechanisms of interaction between active materials and electrolytes.^{40,41} Moreover, contact angle tests provide supporting evidence for the study of wetting procedures.^{24,42,43} Recently,

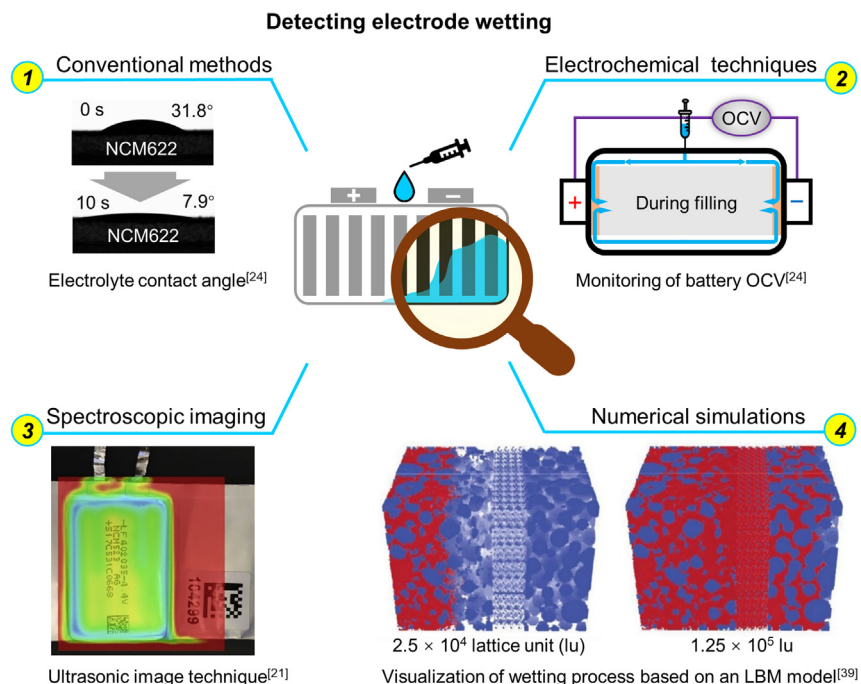


Figure 3. Previous approaches for the characterization and detection of electrode wetting

The detecting methods for electrode wetting can be classified as conventional characterizations, electrochemical methods, *in situ* spectroscopic imaging techniques, and numerical simulations. Electrolyte contact angles and monitoring of battery OCV. Adapted with permission.²⁴ Copyright 2022, Elsevier. Ultrasonic image technique. Adapted with permission.²¹ Copyright 2020, Elsevier. Visualization of the wetting (red) process on an LBM model. Adapted with permission.³⁹ Copyright 2021, Elsevier.

an innovative technique based on in-plane liquid infiltration into a thin porous substrate was proposed by Davoodabadi et al. in which direct visualization of the infiltration front is used for analysis and no mass-to-height conversion is needed.⁴⁴ Because the electrolyte was absorbed horizontally into the electrode through capillary forces, the gravitational influence could be neglected. The authors conducted a series of well-controlled electrolyte infiltration tests on various electrode films using the proposed techniques. A high level of consistency was obtained between the experimental data and the developed analytical model, which demonstrated the robustness and accuracy of the proposed technique.

Electrochemical methods

Electrochemical methods are widely used for battery evaluation due to their advantages of non-destructive, easy operation, and high efficiency. Electrochemical impedance spectroscopy (EIS) is a powerful and non-destructive method for determining the state of LIBs.³ In 2018, Günter et al. took EIS as a proven technique to quantify the degree of wetting in the cell production process.⁴⁵ The results showed that the impedance of the cell depends strongly on the degree of battery wetting and thus can be used to determine the state of complete wetting, which enables faster processing. Our recent work presented an approach to investigate electrode wetting by monitoring the OCV of the $\text{LiNi}_{0.6}\text{Co}_{0.2}\text{Mn}_{0.2}\text{O}_2$ (NCM622)/graphite (Gr) pouch cell based on a high-precision digital recorder.²⁴ It was revealed that the OCV dropped sharply to -0.8 V at the beginning of filling (within 300 ms) and then recovered characteristically to 0.1 V as the wetting process proceeded, which entailed valuable information about the filling mechanisms. The OCV drops to approximately

–0.8 V because the electrolyte filled the current collectors (Al and Cu foils) first. The final value of ~0.1 V was the potential difference between the NCM622 cathode and the Gr anode after fully wetted. The present work provided an effective electrochemically tool to assess the quality of electrolyte filling.

In situ spectroscopic imaging techniques

Visualization of the electrolyte filling process based on *in situ* spectroscopic imaging techniques is an important way to facilitate the understanding of its behavior. In 2016, Knoche et al. pioneered to show that the spreading of the liquid electrolyte inside the battery during the filling and wetting processes was observable by neutron radiography.¹⁹ The distribution of electrolyte liquid over the cell cross-sectional area could be visualized over time. Neutron radiography was also useful for detecting gas entrainment between layers and providing insight into the filling phenomenon. Because ultrasonic transmission is highly sensitive to gas, porosity, and mechanical properties of the materials, it is an alternative spectroscopy technique suitable for detecting battery infiltration. Recently, Deng et al. scanned the battery using a focused ultrasound beam and demonstrated that ultrasound transmission imaging allowed effective measurement of the electrolyte-wetting quality.²¹ The ultrasonic transmission images of fresh and aged cells exhibited very differing ultrasonic transmittance, which could be caused by electrolyte drying due to battery swelling. Gassing, electrolyte drying, and unwetting were observed in aged cells, which helps explain their capacity loss after long-term testing. The proposed ultrasonic imaging technique was quick and inexpensive and was applicable to both large pouches and prismatic cells. Inspired by the use of contrast agents in medicine to enhance X-ray computed tomography (CT) imaging, Chen et al. developed an *in situ* contrast-enhanced four-dimensional (4D) X-ray CT technique to monitor battery wetting by adding contrast agents to the electrolyte, thereby improving the quality of CT imaging.⁴⁶ The contrast-enhanced X-ray CT could effectively enrich the understanding of electrolyte distribution by accurately detecting the electrolyte-wetting state inside the battery stacks and provide practical guidance for improving the uniformity of electrolyte wetting by injection improvements.

Numerical simulations

The visualization of electrode wetting facilitates a deep understanding of infiltration mechanism, whereas it is a challenging task from an experimental perspective. Numerical simulation provides a feasible strategy to alleviate the above issues. Shodiev et al. reported a three-dimensional (3D) resolution lattice Boltzmann method (LBM) model, which was able to simulate the electrolyte filling of porous electrodes.³⁹ The structure model of batteries was obtained from both experiments (micro-X-ray tomography) and computations (coarse-grained molecular dynamics and discrete element method). The model enabled advanced insights into the influence of electrode microstructure on electrolyte infiltration and wetting rates and highlighted the importance of porosity, pore size distribution, and pore interconnectivity on filling dynamics. In addition, the model allowed the visualization of the wetting process. Hagemester et al. developed simulation models based on a computational fluid dynamics (CFD) program to investigate the effects of process parameters, such as pressure and temperature, on the battery dosing and wetting.⁴⁷ The results demonstrated that a low evacuation pressure and a high dosing pressure are beneficial to the dosing process. Studies on the temperature indicated that a low electrolyte temperature and a high gas temperature could slightly increase the amount of electrolyte usage. Recently, Malki et al. proposed a machine learning workflow to study electrode filling.⁴⁸ The approach described by the authors proposed a generic workflow for data analysis and surrogate modeling of electrolyte infiltration parameters

by optimizing design choices. This workflow could also be applied to almost any materials design problem, especially for batteries.

Conventional strategies to promote wetting

Because the pore size of porous electrodes ranges from microns to submicrons, the main driving force for electrolyte wetting of the porous electrodes comes from capillary forces, and the dynamics of wetting are mainly depicted through the Washburn equation,⁴⁹

$$\frac{dl}{dt} = \frac{r^2}{8\eta l} \left(\frac{2\gamma_{LV} \cos \theta}{r} - \Delta p \right) \quad (\text{Equation 4})$$

where l is the distance of liquid electrolyte penetration at time t , r is the radius of the pore inside the electrode, and θ is the contact angle of the electrolyte and electrode particle. η and γ_{LV} are the viscosity of the electrolyte and liquid-to-vapor surface tension, respectively. Δp represents the pressure difference in electrolyte penetration induced by vacuum, pressurization, and gravity. \tilde{r} is utilized as the equivalent radius of the effect caused by the true flow of the electrolyte through the porous electrodes. According to the equation, the existing strategies to promote battery wetting can be classified into two parts: modifying battery components and optimizing operation conditions (Figure 4).

Modifying battery components

Adjusting the porous electrode features is an effective way to accelerate electrolyte immersion from a structural aspect. Davoodabadi et al. studied the influence of calendaring level and wetting temperature on the electrodes produced via organic solvent-based or water-based processes.⁵³ The results indicated that, although increasing the calendaring could enhance the bulk energy density, it usually reduced the wetting rate of electrolyte. The authors demonstrated that switching the manufacturing of anodes from conventional to aqueous processing would slow down the wetting process of electrolytes, whereas switching the cathode manufacturing from organic to aqueous processing would greatly affect the pore structure of cathodes, leading to irregularly shaped wetting zones. In 2014, Pflöging et al. employed laser structuring technique to create capillary microstructures in the tape-cast electrodes, which greatly accelerated the wetting of electrolyte.⁵⁰ The laser-ablated cathode and anode surfaces exhibited regularly ordered concave channels. Compared with the unstructured electrodes, the laser-structured electrodes exhibited significant advantages in terms of capillary climbing ability and wettability, thus shortening the infiltration time of LIBs greatly. Recently, Dunlap et al.⁵⁴ and Habedank et al.⁵⁵ further refined the electrode structures via laser ablation in order to enhance their wettability. The pore size distribution is another parameter that influences electrolyte immersion. Recently, Jeon et al. enhanced the wettability of the electrodes by controlling the volume ratio of particles with different sizes.⁵⁶ The results revealed that the particle-size ratio and porosity have a strong impact on the wettability of electrodes. The distribution of electrolyte and the associated distribution of pore size not only affected the wetting behavior but also comprised a key factor in determining the wetting rate. Shodiev et al. performed permeation simulations based on the LBM to analyze the electrolyte saturation as a function of time.⁴ The authors proposed the use of structures with layers that have different pore network properties as a potential method for tuning the wettability of the electrode layers in batteries.

In addition, ceramic-coated membrane separators, which were fabricated by deploying a ceramic-coated layer (CCL) on the separators, have also been used to

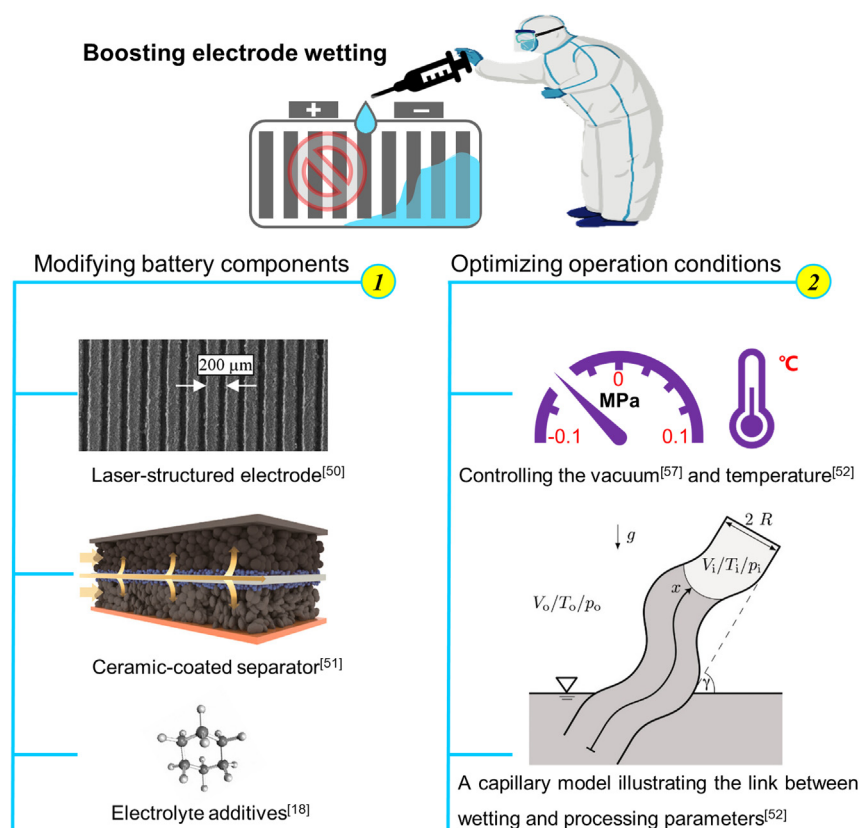


Figure 4. Current strategies to promote electrode wetting

The strategies to promote wetting can be classified into two parts: modifying battery components and optimizing operation conditions. SEM image of the laser-structured electrodes. Adapted with permission.⁵⁰ Copyright 2014, Royal Society of Chemistry. Illustration of electrolyte wetting in a cell assembled with ceramic-coated separators. Adapted with permission.⁵¹ Copyright 2022, American Chemical Society. Schematic illustration of a capillary model that elucidated the relationship between wetting and processing parameters. Adapted with permission.⁵² Copyright 2022, Elsevier.

improve wettability.²⁴ Recently, Jeon et al. presented a mechanistic investigation on the effect of CCL on the electrode wettability and recommended the optimal position of CCL in LIBs.⁵¹ The results showed that, as the liquid electrolyte passed through the CCL, the small pores in the CCL drove the velocity vector farther, resulting in an increased capillary pressure that pushed the liquid toward the electrode, thereby increasing the wetting rate. Wetting agents would be available when the electrolyte was unable to wet the battery rapidly and adequately. Wang et al. described that the addition of cyclohexane (2%~5%) to the control electrolyte resulted in a higher reversible capacity and Coulomb efficiency in the first cycle of the graphite/Li cell and suggested that this improvement might be due to the improved wettability of electrolyte to the separators and electrodes, thus improving the utilization of the electrode material.¹⁸

Optimizing operation conditions

Altering external field conditions, for example, by pressure control, can effectively enhance electrolyte-wetting speed.⁵⁷ Besides, appropriate increases in temperature during the battery filling process can reduce electrolyte viscosity η and improve the wetting ability of the electrolyte. Furthermore, applying vacuum and pressurization to control the external driving force Δp can accelerate the electrolyte flow

speed. Recently, Günter et al. investigated the effects of pressure and temperature in the dosing and wetting process and presented a simple capillary-based model that elucidated the relationship between wetting and the processing parameters.⁵² The model was based on a closed meandering capillary tube, where the rise of the liquid inside the tube was derived analytically and solved numerically. To be industrially relevant, all experiments were performed on cells with capacities above 20 Ah. The results demonstrated a remarkable improvement of the wetting rate at elevated temperatures, low dosing pressures, and intermediate wetting pressures.

Although these methods can improve the wettability of porous electrodes in LIBs, there are many issues to be considered for immersion improvement in high-specific-energy batteries. Modifying battery components improves the wettability of batteries while simultaneously presenting new challenges in battery manufacturing and performance. External effects, such as temperature control and air pressure management, not only enhance electrolyte flow and wetting speed in the porous structures inside electrodes but also allow for convenient operation and universality in various designed battery forms. Therefore, it is of urgency and importance to seek new theories and approaches to accelerating battery wetting. Considering the effect of electric interactions between electrodes and ions in the electrolytes and the structure of commercial cells, regulating the electric field by adjusting the voltage has great potential to enhance the battery infiltration process. Based on this, we explore the mechanism of electrocapillary and the feasibility of utilizing this method for promoting the wettability of electrolytes in porous electrodes of LIBs.

ACCELERATING ELECTRODE WETTING VIA ELECTROCAPILLARY

The definition of electrocapillarity recommended by the International Union of Pure and Applied Chemistry (IUPAC) is “the dependence of interfacial tension on the interphase electrical state.” The electrocapillary phenomenon involves three key elements, including electrodes, electrolyte, and external voltage, which are fully consistent with the characteristics of battery chemistry, thus affording it the potential to be used to accelerate battery wetting.

Basics of electrocapillary phenomenon

A schematic for electrocapillary is shown in [Figure 5A](#)—when an external voltage is applied between the electrolyte and electrode, an induced electric field appears at the dielectric layer and disturbs the electrostatic interactions of the adsorption species in the dielectric layer.²⁵ Thus, the wettability of the electrolyte on the electrode could be modified due to the improved adsorption of ions by the effect of electric interaction, and the contact angle decreased.⁵⁸ As shown in [Figure 5B](#), the concentration of the electrolyte and the applied voltage have a significant influence on the interaction between the electrolytes, which can be represented by the interfacial surface tension γ_{SL} . First, the equilibrium constant of ions (pK or pH) determined by the electrolyte system and concentration has an impact on the charges absorbed by electrodes. When the surface charges in the shearing plane are zero, the pK or pH of the electrolyte can be defined as the point of zero charge (PZC).⁵⁹ At this point, γ_{SL} reaches a maximum in a certain range due to weakened electric interactions. In addition, although the electrolyte system and concentration are fixed, the applied voltage can change γ_{SL} and reach the maximum value by changing the electrode surface to the zero-excess electronic (free charge) state. This voltage is called the potential of zero charge and marked as Φ_{PZC} .

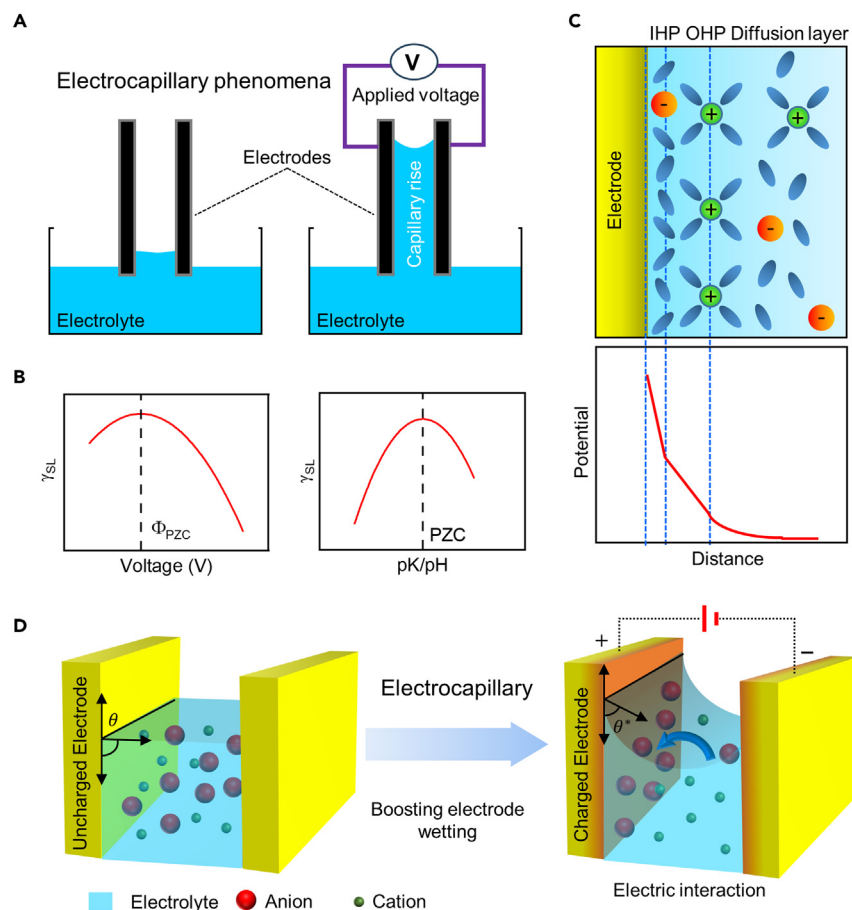


Figure 5. Fundamentals of the electrocapillary phenomenon and its validation for boosting electrode wetting

(A) Illustration of electrocapillary phenomenon that involves electrodes, electrolyte, and applied voltage.
 (B) Influence of electrolyte concentration and external voltage on electrowetting.
 (C) Double-layer structure and potential of the interface between the electrode and electrolyte.
 (D) Numerical simulation of the enhancement in the electrode immersion rate by applying an external voltage.

According to Stern's model, the interfacial layer (Figure 5C) can be divided into the inner Helmholtz plane (IHP), outer Helmholtz plane (OHP), and diffusion layer.^{60,61} The IHP consists of the specific adsorption of ions or solvent molecules on the surface of electrodes, whereas the OHP contains solvated ions, and desolvation processes occur here. Farther from the surface, the diffusion layer marks the transition from the OHP to the bulk electrolyte and has a changing concentration of solvent molecules and solvated ions. At the OHP, a shearing plane contains components with specific affinity to the electrode surface, and other ions or solvent molecules can move freely outside of it. In this plane, the absorbed ions and electrode charges result in a potential difference, and the potential at the plane is the so-called zeta potential in colloid theory. Because of the enrichment of charges at the double layer and the electric interactions with ions in the electrolyte, the trend in liquid contraction here is suppressed, and then the interactions between the electrode and electrolyte are decreased, which reduces the contact angle and raises the height of liquid electrolyte inside the porous electrodes (Figure 5D).

Electrocapillary is a phenomenon included in the theory of electrowetting. In 1969, Dahms introduced the electrowetting-on-dielectric (EWOD) configuration by using an insulating layer to separate the aqueous phase from the electrode, which effectively prevented the occurrence of electrolysis and laid the foundation for its commercial applications.⁶² Subsequently, electrowetting has been used in diverse applications, such as lab-on-a-chip, point-of-care, biomedical, chemical, optical, robotics, and electrical machines. Nowadays, electrowetting has been successfully commercialized for applications in digital microfluidics and optical devices (tunable lenses and electronic displays).

Electrocapillary for accelerated electrode wetting

For commercial LIBs, the electrodes consist of porous structures consisting of active material particles, and the electrolyte consists of lithium salts (such as 1 M LiPF₆) dissolved in organic solvents (such as carbonate ester). To quantitatively study the conditions for the realization of the electrowetting effect in porous electrodes of LIBs, the quantified theoretical equation for electrocapillary and actual parameters should be confirmed. The relationship for initial contact angle θ and the contact angle after applied voltage θ^* can be described by the Lippmann equation⁶³:

$$\cos \theta^* = \cos \theta + \frac{1}{2\gamma_{LV}} \frac{\epsilon\epsilon_0}{d} (\Phi - \Phi_{PZC})^2 \quad (\text{Equation 5})$$

where d is the Debye length and ϵ and ϵ_0 are the relative permittivity and vacuum permittivity, respectively. γ_{LV} is the surface tension of the electrolyte, Φ is the applied voltage between the electrode and electrolyte, and Φ_{PZC} is the potential of zero charge. The surface tension γ_{LV} of the common electrolyte is about 36.5 nN m^{-1} , the dielectric constant (relative and vacuum permittivity) $\epsilon\epsilon_0$ is approximately $19 \times 8.854 \times 10^{-12} \text{ F m}^{-1}$, and the Debye length d of the porous electrode double layer is approximately $0.3 \sim 1 \text{ nm}$.^{64–66} For the commonly used active material particles, the potential of zero charge Φ_{PZC} is approximately at the millivolt level.⁶⁷ Combined with the Lippmann equation, the results show that the order of magnitude applied voltage for realizing electrowetting in commercial LIBs is suitable for operation with a magnitude of $0.1 \sim 1 \text{ V}$.

As presented in [Figure 6A](#), the wetting curves of porous electrodes with different applied voltages are investigated using numerical simulations in conjunction with the Washburn equation (see [experimental section](#) in [supplemental information](#)). Compared with no external voltage, the applied voltage decreases the normalized electrolyte-wetting time significantly under the normalized immersion distance, and the higher voltage shows better results. The characteristic wetting time decreases from 4.48 to 3.95, 2.92, or 2.04 when the external voltage is set to 0.1, 0.2, or 0.3 V, respectively. On the basis of the above theoretical analysis, it is feasible to boost electrode wetting by means of electrocapillary.

To further verify the effect of electrocapillary in promoting battery immersion, *in situ* ultrasonic imaging detection ([Figure S1A](#) in [supplemental information](#)) was used to monitor the immersion status of 3.1 Ah LiFePO₄ (LFP)/graphite (Gr) pouch cells with applied voltage (see [experimental section](#) in [supplemental information](#); [Table S1](#)). The LFP/Gr pouch cells were evaluated with and without an external voltage of 0.1 V, which are marked as V-Cell and control cell, respectively. The ultrasonic imaging results for the V-Cell and control cell are obtained after being wetted 1, 2, and 5 h ([Figure 6B](#)). As the immersion time increased, the wetted area (shown as green) spread and the nonwetted area (shown as blue) contracted, but the ultrasonic imaging results of both the V-Cell and control cell varied

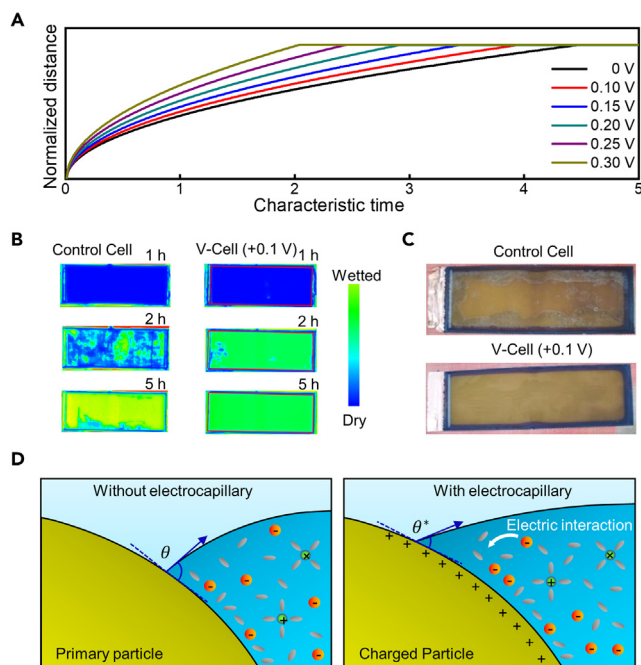


Figure 6. Simulations and experimental validations for electrocapillary promoting electrode wetting

- (A) Numerical simulation of the enhancement in the electrode immersion rate by an external voltage.
- (B) Comparison of ultrasonic imaging results of injected control cell (no external voltage) and V-Cell (with 0.1 V external voltage).
- (C) Different lithium precipitation behaviors on the Gr anodes for the control cell and V-cell after the formation process.
- (D) Schematic of the electrocapillary mechanism on the active electrode particle surface.

dramatically. Within 2 h of filling, the V-Cell was almost completely wetted, whereas the control cell still exhibited many unwetted zones. After 5 h of filling, the V-Cell was totally wetted, but the control cell still remained with a number of unwetted sections. At this time point, both of these cells were converted to the formation process. After the first charging at 0.1 C, the V-Cell and control cell were disassembled, and the anode slices were compared, as shown in [Figure 6C](#). The anode of the V-Cell exhibited significant lithium plating around the edge, whereas the anode of the control cell was clean and showed uniform gold color of charged graphite. The comparison shows that regulation of the external voltage can effectively promote the wetting process, whereas the well-wetted cell can effectively suppress lithium precipitation caused by incomplete wetting. The following factors may contribute to the phenomenon of Li plating. First, there may not be enough available space to accommodate the Li^+ from the corresponding area of LFP cathode if parts of the graphite anode are not fully wetted, which will result in localized Li plating. Second, the residual gases inside the electrode may block the uniform insertion of Li^+ . Third, electrodes that are not sufficiently wetted have higher internal resistance, which tends to lead to higher overpotentials, and thus are more likely to cause Li plating.

To confirm the interacting form with the external voltage, a linear scanning voltammetry test was performed at 0.05, 0.1, and 1 mV s^{-1} , which corresponded to charging rates of 0.13, 0.25, and 2.5 C, respectively ([Figure S1B](#)). When the

voltage was under approximately 1 V, the current was low, and the electric interaction dominated. However, SEI formation took place above 1 V with the reaction current.³⁵ These results indicate that the improved wetting originated from the enhanced electric interaction due to the external voltage. Based on the above results and discussion, the electrocapillary mechanism during the electrolyte immersion process inside the porous electrodes is shown in [Figure 6D](#). As the electrolyte is immersed during battery infiltration, the wetting front of the liquid penetrates into the porous electrode and makes contact with the active material particles. The applied external voltage can sufficiently promote the electrolyte immersion process, demonstrated as proven by theoretical analysis and experimental verification. The charged electrode particles showed increased electric interactions with electrolytes, leading to a lower contact angle and better wetting of electrodes. As a consequence, the wetting speed and wetting uniformity are strongly promoted, which reveal the great impact of electrocapillarity on battery filling process.

CONCLUSION AND PERSPECTIVE

Electrolyte filling is a quality-critical and cost-intensive process in battery production, especially for high-energy batteries employing thick and highly compressed electrodes. In this perspective, first, the fundamental principles and characterization approaches involved in electrode wetting, which include conventional surface analysis methods, electrochemical methodologies, and *in situ* spectroscopic imaging techniques, are outlined. Second, the basics of the electrocapillary phenomena and the key elements (electrodes, electrolytes, and voltages) involved in the phenomena are carefully overviewed. In addition, the combination of the Lippmann equation with numerical simulations postulates that it is feasible to employ electrocapillarity to boost the electrode wetting. Then we pioneer to demonstrate the electrocapillarity effect on electrolyte wetting and preliminarily verify its applicability in speeding the battery filling process. Targeting the electrode wetting challenges faced by high-energy LIBs, this work offers a strategy to enhance electrode wettability based on electrocapillary theory, which will enrich the design philosophy and promote the production efficiency of next-generation batteries.

SUPPLEMENTAL INFORMATION

Supplemental information can be found online at <https://doi.org/10.1016/j.joule.2023.11.012>.

ACKNOWLEDGMENTS

The authors thank the National Natural Science Foundation of China (no. 52206263 [Y.S.], no. U21A20170 [X.H.], no. 52007099 [D.R.], and no. 22279070 [L.W.]) and the Ministry of Science and Technology of China (no. 2021YFB2501900 [D.R.] and 2019YFA0705703 [L.W.]). In addition, the Joint Work Plan for Research Projects under the Clean Vehicles Consortium at U.S. and China-Clean Energy Research Center (CERC-CVC2.0, 2016-2020) and the “Explorer 100” cluster system of Tsinghua National Laboratory for Information Science and Technology for facility support are also thanked by the authors.

DECLARATION OF INTERESTS

The authors declare no competing interests.

REFERENCES

1. Yoshino, A. (2012). The birth of the lithium-ion battery. *Angew. Chem. Int. Ed. Engl.* *51*, 5798–5800.
2. Armand, M., and Tarascon, J.M. (2008). Building better batteries. *Nature* *451*, 652–657.
3. Song, Y., Wang, X., Cui, H., Huang, J., Hu, Q., Xiao, X., Liang, H., Yang, K., Wang, A., Liu, J., et al. (2023). Probing the particle size dependence of nonhomogeneous degradation in nickel-rich cathodes for high-energy lithium-ion batteries. *eTransportation* *16*, 100223.
4. Shodiev, A., Zanutto, F.M., Yu, J., Chouchane, M., Li, J., and Franco, A.A. (2022). Designing electrode architectures to facilitate electrolyte infiltration for lithium-ion batteries. *Energy Storage Mater.* *49*, 268–277.
5. Wood, D.L., Li, J., and Daniel, C. (2015). Prospects for reducing the processing cost of lithium ion batteries. *J. Power Sources* *275*, 234–242.
6. Wu, F., Liu, M., Li, Y., Feng, X., Zhang, K., Bai, Y., Wang, X., and Wu, C. (2021). High-mass-loading electrodes for advanced secondary batteries and supercapacitors. *Electrochem. Energ. Rev.* *4*, 382–446.
7. Li, Y., Song, S., Kim, H., Nomoto, K., Kim, H., Sun, X., Hori, S., Suzuki, K., Matsui, N., Hirayama, M., et al. (2023). A lithium superionic conductor for millimeter-thick battery electrode. *Science* *381*, 50–53.
8. Liu, Y., Zhang, R., Wang, J., and Wang, Y. (2021). Current and future lithium-ion battery manufacturing. *iScience* *24*, 102332.
9. Morse, I. (2021). A dead battery dilemma. *Science* *372*, 780–783.
10. Liu, J., Bao, Z., Cui, Y., Dufek, E.J., Goodenough, J.B., Khalifah, P., Li, Q., Liaw, B.Y., Liu, P., Manthiram, A., et al. (2019). Pathways for practical high-energy long-cycling lithium metal batteries. *Nat. Energy* *4*, 180–186.
11. Zhan, R.M., Ren, D.S., Liu, S.Y., Chen, Z.X., Liu, X.R., Wang, W.Y., Fu, L., Wang, X.C., Tu, S.B., Ou, Y.T., et al. (2023). A paradigm of calendaring-driven electrode microstructure for balanced battery energy density and power density. *Adv. Energy Mater.* *13*, 2202544.
12. Sauter, C., Zahn, R., and Wood, V. (2020). Understanding electrolyte infilling of lithium ion batteries. *J. Electrochem. Soc.* *167*, 7, 100546.
13. Biesheuvel, P.M., Fu, Y., and Bazant, M.Z. (2011). Diffuse charge and Faradaic reactions in porous electrodes. *Phys. Rev. E Stat. Nonlin. Soft Matter Phys.* *83*, 61507.
14. Knehr, K.W., Hodson, T., Bommier, C., Davies, G., Kim, A., and Steingart, D.A. (2018). Understanding full-cell evolution and non-chemical electrode crosstalk of Li-ion batteries. *Joule* *2*, 1146–1159.
15. Feng, X.N., Zheng, S.Q., Ren, D.S., He, X.M., Wang, L., Cui, H., Liu, X., Jin, C.Y., Zhang, F.S., Xu, C.S., et al. (2019). Investigating the thermal runaway mechanisms of lithium-ion batteries based on thermal analysis database. *Appl. Energy* *246*, 53–64.
16. Zhu, J., Wierzbicki, T., and Li, W. (2018). A review of safety-focused mechanical modeling of commercial lithium-ion batteries. *J. Power Sources* *378*, 153–168.
17. An, S.J., Li, J., Daniel, C., Mohanty, D., Nagpure, S., and Wood, D.L. (2016). The state of understanding of the lithium-ion-battery graphite solid electrolyte interphase (SEI) and its relationship to formation cycling. *Carbon* *105*, 52–76.
18. Wang, X., Naito, H., Sone, Y., Segami, G., and Kuwajima, S. (2005). New additives to improve the first-cycle charge–discharge performance of a graphite anode for lithium-ion cells. *J. Electrochem. Soc.* *152*, A1996.
19. Knoche, T., Zinth, V., Schulz, M., Schnell, J., Gilles, R., and Reinhart, G. (2016). In situ visualization of the electrolyte solvent filling process by neutron radiography. *J. Power Sources* *331*, 267–276.
20. Schilling, A., Gümbel, P., Möller, M., Kalkan, F., Dietrich, F., and Dröder, K. (2019). X-ray based visualization of the electrolyte filling process of lithium ion batteries. *J. Electrochem. Soc.* *166*, A5163–A5167.
21. Deng, Z., Huang, Z., Shen, Y., Huang, Y., Ding, H., Luscombe, A., Johnson, M., Harlow, J.E., Gauthier, R., and Dahn, J.R. (2020). Ultrasonic scanning to observe wetting and “Unwetting” in Li-ion pouch cells. *Joule* *4*, 2017–2029.
22. Schilling, A., Wiemers-Meyer, S., Winkler, V., Nowak, S., Hoppe, B., Heimes, H.H., Dröder, K., and Winter, M. (2020). Influence of separator material on infiltration rate and wetting behavior of lithium-ion batteries. *Energy Technol.* *8*, 1900078.
23. Lee, S.G., Jeon, D.H., Kim, B.M., Kang, J.H., and Kim, C.-J. (2013). Lattice Boltzmann simulation for electrolyte transport in porous electrode of lithium ion batteries. *J. Electrochem. Soc.* *160*, H258–H265.
24. Cui, H., Ren, D., Yi, M., Hou, S., Yang, K., Liang, H., Feng, X., Han, X., Song, Y., Wang, L., and He, X. (2022). Operando monitoring of the open circuit voltage during electrolyte filling ensures high performance of lithium-ion batteries. *Nano Energy* *104*, 107874.
25. Tan, J., Sun, S., Jiang, D., Xu, M., Chen, X., Song, Y., and Wang, Z.L. (2022). Advances in triboelectric nanogenerator powered electrowetting-on-dielectric devices: mechanism, structures, and applications. *Mater. Today* *58*, 201–220.
26. Zhang, Y., and Nguyen, N.-T. (2017). Magnetic digital microfluidics – a review. *Lab Chip* *17*, 994–1008.
27. Li, L., Liu, C., Ren, H., and Wang, Q.H. (2016). Optical switchable electrowetting lens. *IEEE Photon. Technol. Lett.* *28*, 1505–1508.
28. Kim, D.Y., and Steckl, A.J. (2010). Electrowetting on paper for electronic paper display. *ACS Appl. Mater. Interfaces* *2*, 3318–3323.
29. Brutin, D., and Starov, V. (2018). Recent advances in droplet wetting and evaporation. *Chem. Soc. Rev.* *47*, 558–585.
30. Joud, J.-C., and Barthés-Labrousse, M.-G. (2015). Components of the surface energy. In *Physical Chemistry and Acid-Base Properties of Surfaces* (John Wiley & Sons), pp. 23–36.
31. Zhang, W., Wang, D., Sun, Z., Song, J., and Deng, X. (2021). Robust superhydrophobicity: mechanisms and strategies. *Chem. Soc. Rev.* *50*, 4031–4061.
32. Bormashenko, E. (2015). Progress in understanding wetting transitions on rough surfaces. *Adv. Colloid Interface Sci.* *222*, 92–103.
33. Wang, S., Liu, K., Yao, X., and Jiang, L. (2015). Bioinspired surfaces with superwettability: new insight on theory, design, and applications. *Chem. Rev.* *115*, 8230–8293.
34. Wang, P., Li, C., and Zhang, D. (2022). Recent advances in chemical durability and mechanical stability of superhydrophobic materials: multi-strategy design and strengthening. *J. Mater. Sci. Technol.* *129*, 40–69.
35. Liu, M., Wang, S., and Jiang, L. (2017). Nature-inspired superwettability systems. *Nat. Rev. Mater.* *2*, 17036.
36. Milionis, A., Loth, E., and Bayer, I.S. (2016). Recent advances in the mechanical durability of superhydrophobic materials. *Adv. Colloid Interface Sci.* *229*, 57–79.
37. Nicolau, B.G., Petronico, A., Letchworth-Weaver, K., Ghadar, Y., Haasch, R.T., Soares, J.A.N.T., Rooney, R.T., Chan, M.K.Y., Gewirth, A.A., and Nuzzo, R.G. (2018). Controlling interfacial properties of lithium-ion battery cathodes with alkylphosphonate self-assembled monolayers. *Adv. Materials Interfaces* *5*, 1701292.
38. Sedev, R. (2011). Electrowetting: electrocapillarity, saturation, and dynamics. *Eur. Phys. J. Spec. Top.* *197*, 307–319.
39. Shodiev, A., Primo, E., Arcelus, O., Chouchane, M., Osenberg, M., Hilger, A., Manke, I., Li, J., and Franco, A.A. (2021). Insight on electrolyte infiltration of lithium ion battery electrodes by means of a new three-dimensional-resolved lattice Boltzmann model. *Energy Storage Mater.* *38*, 80–92.
40. Song, Y., Liu, X., Ren, D., Liang, H., Wang, L., Hu, Q., Cui, H., Xu, H., Wang, J., Zhao, C., et al. (2022). Simultaneously blocking chemical crosstalk and internal short circuit via gel-stretching derived nanoporous non-shrinkage separator for safe lithium-ion batteries. *Adv. Mater.* *34*, e2106335.
41. Song, Y., Wang, L., Cui, H., Liang, H., Hu, Q., Ren, D., Yang, Y., Zhang, H., Xu, H., and He, X. (2022). Boosting battery safety by mitigating thermal-induced crosstalk with a bi-continuous separator. *Adv. Energy Mater.* *12*, 2201964.
42. Song, Y.-Z., Yuan, J.-J., Yin, X., Zhang, Y., Lin, C.-E., Sun, C.-c., Fang, L.-F., Zhu, B., and Zhu, L.-P. (2018). Effect of polyphenol-polyamine treated polyethylene separator on the ionic conduction and interface properties for

- lithium-metal anode batteries. *J. Electroanal. Chem.* **816**, 68–74.
43. Song, Y.-Z., Zhang, Y., Yuan, J.-J., Lin, C.-E., Yin, X., Sun, C.-C., Zhu, B., and Zhu, L.-P. (2018). Fast assemble of polyphenol derived coatings on polypropylene separator for high performance lithium-ion batteries. *J. Electroanal. Chem.* **808**, 252–258.
44. Davoodabadi, A., Li, J., Liang, Y., Wood, D.L., Singler, T.J., and Jin, C. (2019). Analysis of electrolyte imbibition through lithium-ion battery electrodes. *J. Power Sources* **424**, 193–203.
45. Günter, F.J., Habedank, J.B., Schreiner, D., Neuwirth, T., Gilles, R., and Reinhart, G. (2018). Introduction to electrochemical impedance spectroscopy as a measurement method for the wetting degree of lithium-ion cells. *J. Electrochem. Soc.* **165**, A3249–A3256.
46. Chen, H.-S., Yang, S., Song, W.-L., Yang, L., Guo, X., Yang, X.-G., Li, N., and Fang, D. (2023). Quantificational 4D visualization and mechanism analysis of inhomogeneous electrolyte wetting. *eTransportation* **16**, 100232.
47. Hagemester, J., Günter, F.J., Rinner, T., Zhu, F., Papst, A., and Daub, R. (2022). Numerical models of the electrolyte filling process of lithium-ion batteries to accelerate and improve the process and cell design. *Batteries* **8**, 159.
48. El Malki, A., Asch, M., Arcelus, O., Shodiev, A., Yu, J., and Franco, A.A. (2023). Machine learning for optimal electrode wettability in lithium ion batteries. *J. Power Sources Adv.* **20**, 100114.
49. Lei, J., Xu, Z., Xin, F., and Lu, T.J. (2021). Dynamics of capillary flow in an undulated tube. *Phys. Fluids* **33**, 52109.
50. Pflöging, W., and Pröll, J. (2014). A new approach for rapid electrolyte wetting in tape cast electrodes for lithium-ion batteries. *J. Mater. Chem. A* **2**, 14918–14926.
51. Jeon, D.H., Song, J.-H., Yun, J., and Lee, J.-W. (2022). Mechanistic insight into wettability enhancement of lithium-ion batteries using a ceramic-coated layer. *ACS Nano* **17**, 1305–1314.
52. Günter, F.J., Keilhofer, J., Rauch, C., Rössler, S., Schulz, M., Braunwarth, W., Gilles, R., Daub, R., and Reinhart, G. (2022). Influence of pressure and temperature on the electrolyte filling of lithium-ion cells: experiment, model and method. *J. Power Sources* **517**, 230668.
53. Davoodabadi, A., Li, J., Zhou, H., Wood, D.L., Singler, T.J., and Jin, C. (2019). Effect of calendaring and temperature on electrolyte wetting in lithium-ion battery electrodes. *J. Energy Storage* **26**, 101034.
54. Dunlap, N., Sulas-Kern, D.B., Weddle, P.J., Usseglio-Viretta, F., Walker, P., Todd, P., Boone, D., Colclasure, A.M., Smith, K., Tremolet de Villers, B.J., and Finegan, D.P. (2022). Laser ablation for structuring Li-ion electrodes for fast charging and its impact on material properties, rate capability, Li plating, and wetting. *J. Power Sources* **537**, 231464.
55. Habedank, J.B., Günter, F.J., Billot, N., Gilles, R., Neuwirth, T., Reinhart, G., and Zaeh, M.F. (2019). Rapid electrolyte wetting of lithium-ion batteries containing laser structured electrodes: in situ visualization by neutron radiography. *Int. J. Adv. Manuf. Technol.* **102**, 2769–2778.
56. Jeon, D.H. (2021). Enhancing electrode wettability in lithium-ion battery via particle-size ratio control. *Appl. Mater. Today* **22**, 100976.
57. Weydanz, W.J., Reisenweber, H., Gottschalk, A., Schulz, M., Knoche, T., Reinhart, G., Masuch, M., Franke, J., and Gilles, R. (2018). Visualization of electrolyte filling process and influence of vacuum during filling for hard case prismatic lithium ion cells by neutron imaging to optimize the production process. *J. Power Sources* **380**, 126–134.
58. Costa, R., Pereira, C.M., and Silva, F. (2010). Double layer in room temperature ionic liquids: influence of temperature and ionic size on the differential capacitance and electrocapillary curves. *Phys. Chem. Chem. Phys.* **12**, 11125–11132.
59. Schmickler, W. (1996). Electronic effects in the electric double layer. *Chem. Rev.* **96**, 3177–3200.
60. Oldham, K.B. (2008). A Gouy–Chapman–Stern model of the double layer at a (metal)/(ionic liquid) interface. *J. Electroanal. Chem.* **613**, 131–138.
61. Yan, C., Yuan, H., Park, H.S., and Huang, J.-Q. (2020). Perspective on the critical role of interface for advanced batteries. *J. Energy Chem.* **47**, 217–220.
62. Dahms, H. (1969). Electrocapillary measurements at the interface insulator-electrolytic solution. *J. Electrochem. Soc.* **116**, 1532.
63. Shamai, R., Andelman, D., Berge, B., and Hayes, R. (2007). , Electricity, and between... On electrowetting and its applications. *Soft Matter* **4**, 38–45.
64. Dahbi, M., Violleau, D., Ghamouss, F., Jacquemin, J., Tran-Van, F., Lemordant, D., and Anouti, M. (2012). Interfacial properties of LiTFSI and LiPF₆-based electrolytes in binary and ternary mixtures of alkylcarbonates on graphite electrodes and Celgard separator. *Ind. Eng. Chem. Res.* **51**, 5240–5245.
65. Li, L., Xu, G., Zhang, S., Dong, S., Wang, S., Cui, Z., Du, X., Wang, C., Xie, B., Du, J., et al. (2022). Highly fluorinated al-centered lithium salt boosting the interfacial compatibility of Li-metal batteries. *ACS Energy Lett.* **7**, 591–598.
66. Self, J., Hahn, N.T., and Persson, K.A. (2022). Solvation effects on the dielectric constant of 1 M LiPF₆ in ethylene carbonate: ethyl methyl carbonate 3:7. *Energy Environ. Mater.* **0**, e12494. <https://doi.org/10.1002/eem2.12494>.
67. Para, M.L., Versaci, D., Amici, J., Caballero, M.F., Cozzarin, M.V., Francia, C., Bodoardo, S., and Gamba, M. (2021). Synthesis and characterization of montmorillonite/polyaniline composites and its usage to modify a commercial separator. *J. Electroanal. Chem.* **880**, 114876.